UNIVERSITY OF MINNESOTA
ST. ANTHONY FALLS LABORATORY
Engineering, Environmental and Geophysical Fluid Dynamics

Project Report No. 527

Wind Velocity Measurements on Two Small Ice-Covered Lakes:

A Compilation of Data with Some Results and Discussion

By

James W. Thill

Compiled by
Corey D. Markfort

January 2009

Minneapolis, Minnesota

Abstract

This report gives a compilation of wind velocity measurements on Round Lake and Lake Harriet taken over the ice in 2004 and 2005. Results, primarily from the 2004 Round Lake study, are presented and discussed to characterize the wind sheltering effect of tree canopies on lakes. Wind forcing is important for predicting many physical, chemical and biological lake processes, and there is a lack of understanding of the spatial and temporal variation of wind speeds over lakes especially those sheltered by canopies. The objective of this study was to evaluate, with observations, the spatial evolution of an internal wind boundary layer as it flows from a rough canopy of trees and shoreline reeds onto an ice cover of a lake. More specifically, the study sought to determine the streamwise profile of the shear stress on a lake surface, and to establish a relationship between surface shear stress and fetch. The data show that reduced wind shear stress extends across approximately half the diameter of Round Lake (~ 500 m).

Table of Contents

1. Introduction

The surface mixed layer (SML) of lakes is the most dynamic zone within the limnological system. Turbulent mixing in the SML is the primary facilitating mechanism of transport of momentum, heat, and mass from the air-water interface into the water. Surface mixed layer deepening destroys stratification. Stratification is known to limit gas transfer (most notably, O_2) in the water column of lakes and reservoirs and affect the sediment chemistry (Condie and Webster 2001; Hocking and Patterson 1994; Portielje and Lijklema 1995; Kolb and Heineman 1995). In engineered aquatic systems constructed for contaminant removal, such as stormwater pollution control ponds and wetlands, stratification is generally considered undesirable (Lawrence and Breen 1998). Surface layer turbulent mixing, and its effects on stratification, is a crucial underpinning of our understanding of many ecological, geochemical, and physical processes that occur in lakes. Wind stress and free thermal convection at the water surface are the main processes that generate SML turbulence. Of these, the wind stress is much less well understood (Wüest and Lorke 2003).

While arguably among the most important forces in the hydrodynamic balance of the limnological system, wind stress on the surface of a small water body is not well documented. Direct observations of wind over or near lakes are not only uncommon but also questionable because of uncertainty about the spatial inhomogeneity of the instantaneous and time averaged wind field. More common are measurements at local weather stations, typically several kilometers from the lake of interest. Often these measurements bear little predictable correlation with wind speeds directly over lakes. This lack of observation necessitates that numerical lake models for water quality calibrate wind speed by an unknown parameter referred to as the "wind sheltering coefficient" (Hondzo and Stefan, Fang and Stefan). The calibrated wind speed is unlikely to represent wind speed at a particular point in space and time; rather the calibration provides an areally and temporally averaged wind speed that minimizes the mean residual between the model results and data. While practical for zero or one-dimensional lake models, this approach neglects meaningful and significant details of non-uniform wind speed distributions over

lakes that are likely to be important for the construction of physically realistic three-dimensional lake models (e.g. Edinger 2001, Wang and Hutter 1998; Wang, Hutter, and Bäuerle 2001; Wang 2003), for example.

Lakes are generally situated in topographic depressions and surrounded by vegetation or man-made structures that shelter them from the wind. This sheltering reduces the speed of the wind that impinges on the water surface. Since momentum and mechanical energy flux across the air-water interface scale at rates proportional to the wind speed squared and cubed, respectively, even small spatial variations in surface wind speed can be expected to produce comparatively large spatial variations in wind-driven flows and turbulent transport within a lake (Melville, 1996). In a more general sense, the sensitivity of the surface fluxes to wind speed makes an accurate determination wind field over a lake highly desirable.

From a lake modeling perspective, the wind speed over a lake is an uncertain parameter that must be inferred from local wind data, which is commonly measured several kilometers or more from the lake of interest. This is typically accomplished by using a wind speed coefficient to modify the wind speed value recorded at the local weather station such that it more closely represents the wind speed at the lake (Hondzo and Stefan, Fang and Stefan). Often, this coefficient cannot easily be determined *a priori*, and is generally found by way of some optimization scheme that best fits the model to observations. The wind speed values determined in this way represent a spatially averaged wind speed that may not be representative of the wind speed at any given point over the lake surface.

To assess the wind sheltering of a lake we have to study the atmospheric flow over an irregular topography if the lake is surrounded by hilly terrain, and the surface roughness transition from vegetation on land or in wetlands to the water surface, if a lake is located in a flat terrain. In some cases topography and roughness transition will both have to be considered, and in urban areas buildings on the shoreline of a lake may also have an important influence on wind sheltering.

The effect of roughness transitions on atmospheric boundary layer flow is still poorly understood. Although atmospheric flows are continuously subjected to such transitions over the greater part of terrestrial Earth, few field measurements have been executed to study them and numerical solutions are, for the most part, in their infancy. Moreover, the flow downwind of a plant canopy is more complicated than a simple roughness transition since it also involves a wake in the presence of the transition. This wake is the result of a lower layer of relatively low velocity air that emerges from the tree canopy and a region of higher velocity air flowing from above the canopy. At the trailing edge of the canopy, and over the lake surface, the interaction of these two layers of contrasting velocity produces a shear layer and an as yet undetermined downward flux of momentum.

The objective of this study was to evaluate, with observations, the spatial evolution of an internal wind boundary layer as it flows from a rough canopy of trees and shoreline reeds onto an ice cover on a lake representative. More specifically, we sought to determine the streamwise profile of the shear stress on the lake surface, and to establish a relationship between surface shear stress and fetch.

2. Study site selection and characteristics

Wind sheltering of a lake is a function of local topography, shoreline development, and vegetation. It was desired for Part 1 of this study to evaluate only the effects of shoreline vegetation, isolating this effect, to the greatest degree possible, from the effects of topography and shoreline development. With this objective in mind, Round Lake (Area ~1.1 km^2, Figure 1), near Anoka, Minnesota, was selected as the site for this study because it lies in an area of flat topography and has a relatively small amount of shoreline development. As can be seen in Figure 1, Round Lake Boulevard and a small residential subdivision line the lake's southeastern edge. Another residential subdivision lies farther to the southwest. The remainder of the shoreline is generally undeveloped, and the terrain surrounding Round Lake is very flat, and covered by trees (generally < 10 m in height) and marsh grasses. In Figure 2, the heavy black line delineates the approximate boundary between the shoreline grasses and the upland area that is covered by trees. Furthermore, Round Lake, as its name suggests, has a generally circular shape. This circular shape minimizes local flow anisotropies (e.g. because of wind channeling in elongate basins). Finally, Round Lake is shallow and muddy and, therefore, not a popular destination for fishing and other recreational uses. This is an important characteristic because fishermen represent a transient and uncontrollable source of aerodynamic roughness that can jeopardize the quality of experimental results.

For Part 2 of this study it was desired to collect data that show the effects of shoreline topography and development. Lake Harriet (Area ~1 km^2, Figure 2g), in Minneapolis, Minnesota, was selected as the site for this study because it has full shoreline development with large residential houses and mature trees, except on the north side, and a steep bluff of approximately 20-30 m elevation above lake level.

The difficult logistics of working from a water surface often present problems for researchers working on lakes. The northern climate presents an opportunity to work on a stable ice layer that forms on the surface of lakes during the winter. Working on the ice surface has several advantages. The ice cover provides a stable platform; it also allows easy

access to the very edge of a lake surrounded by emergent vegetation or brush wetland. The transition from the atmospheric boundary layer from the vegetation characteristic of the land surface or a wetland can be more easily studied from an ice-surface. The seasonal variations in vegetation characteristics (e.g. leaf area index) can, in principal, be taken into account in the analysis. For practical purposes, however, for a sufficiently large shelter belt (measured parallel to the flow direction of the wind), the permeability of the canopy becomes less important.

3. Field Instrumentation and Procedure

Field measurements were made in February and March 2004 and in February 2005 on Round Lake and in January 2005 on Lake Harriet.

The objective of this field experiment was to obtain vertical profiles of wind speed at multiple locations on the lake surface. Three stations were established. Station 1 was installed near the center of the lake as a reference. Station 2 was installed in different fixed locations on different days. Station Mi was attached to a sled that was periodically moved to a different location (i) on the lake; the locations are denoted by M1, M2, M3, etc, with the 'M' signifying that the station was 'mobile'. Figures 2(a) to 2(d) show the measurement locations on different days.

3.1. Round Lake 2004

The experimental apparatus at each station consisted of three Met One model 014-A wind speed sensors (cup anemometers) mounted at various heights on each of three 2.5 m vertical masts (Figure 3). The cup anemometers were calibrated initially according to the manufacturer's recommended calibrations. Later, we validated these calibrations against a pitot tube in the boundary layer wind tunnel at Saint Anthony Falls Lab. In the velocity intervals of interest, the manufacturer's calibrations were within a few percent, at most, of our independent calibrations. It was found that our computed values of shear stress were for the most part insensitive to these small differences in calibration parameters. For simplicity and consistency, we opted to use the manufacturer's calibration. The heights of the sensors on each mast measure from the top of the ice/snow cover on the lake are provided in Table 1. The lowest sensor was mounted at a height of 0.3-0.5 m, the middle sensor at a height of 0.8-1.2 m, and the highest sensor at a height of 2.2-2.5 m. A Wind Sentry wind direction sensor (manufactured by R.M. Young) was attached to two of the masts at a height of 1.8 m. In all cases, the wind speed and direction were evaluated as 10-second averages. On 21-Feb and 28-Feb-2004, the ten second data were averaged and recorded at 2-minute intervals (this was a wholly unnecessary attempt to save data storage).

On all subsequent measurement days, the raw 10-second wind speed average data were recorded. The data were logged on a Campbell Scientific CR-10X data logger.

3.2. Lake Harriet 2005

After reviewing the results of our analysis from Round Lake 2004, it was deemed necessary to increase the vertical resolution of measurement of the velocity profiles. At sufficiently long fetches, presumably, the boundary layer will be well-developed up to the height of the highest wind speed sensor. In such instances, the velocity profile will exhibit a high degree of linearity when plotted against ln z. At shorter fetches, however, this may not necessarily be the case. This lack of attention to detail was a shortcoming of our initial attempts at characterizing lake surface boundary layer development.

On 23-January, 2005, we visited Lake Harriet armed with larger sensor arrays than we used previously. At Station 1, which was more than a kilometer downwind of the land-lake transition, three Met One 014-A wind speed sensors and a R.M. Wind Sentry wind direction vane were installed (see Table 2 for instrument heights at all stations). Station 2, which was a "mid-lake" station, carried a similar array to Station 1, except for the addition of a fourth 014-A wind speed sensor. The mobile station carried five 014-A wind speed sensors and no instrument for measuring wind direction. We increased the number of wind speed sensors with decreasing fetch in hopes of being able to capture the smaller scale characteristics of the velocity profile after the transition.

All wind speed measurements were recorded as 10-second averages. Wind direction measurements were recorded as instantaneous values every 10 seconds.

3.3. Round Lake 2005

On 5-February, 2005, the instrument allocation was similar to that at Lake Harriet on 23-January. Station 1, on the downwind side of the lake, was outfitted with three 014-A wind speed sensors and one Wind Sentry wind direction sensor (See Table 3 for heights of all instruments from Round Lake 2005). Station 2, at "mid-lake", was outfitted with four

wind speed sensors and no direction sensors. The mobile station was outfitted with five wind speed sensors and no direction sensors.

On 17-February, we increased our vertical resolution again by installing five 014-A wind speed sensors at each of the three stations (again, see Table 3 for specific sensor arrangements). Station 1 and Station 2 were outfitted with wind direction sensors.

As on 23-January, all wind speed measurements were recorded as 10-second averages. Wind direction measurements were recorded as instantaneous values every 10 seconds.

4. Field data and analysis procedure

Examples of the raw data from the cup anemometers and the wind direction vanes are plotted in Figures 4(a) and 4(b).

The first step in the data analysis was the determination of an integral time scale by an autocorrelation analysis on the 10-second or 2-minute wind speed data measured by the 014-A cup anemometers.

The second step was to calculate 20-minute averages of the recorded 2-minute or 10-second velocity data as well as standard deviations. Twenty minutes provides an average of ten 2-minute data points or 120 10-second data points, and is considerably longer than both the integral time scale of the data (about 3 minutes), and the travel time of a wind gust across the entire lake at 5m/s wind speed (also about 3 minutes).

The 20-minute average wind speeds *u(z)* were plotted as a function of *ln z* where z = elevation above the ice/snow surface. This plot would be linear for a 'classical' turbulent boundary layer velocity distribution, with slope and intercept corresponding to the shear velocity u_* and the aerodynamic roughness length z_0, respectively. The equation of the semi-logarithmic distribution that is often used to describe velocity profiles in a near-surface turbulent boundary layer is

$$u(z) = \frac{u_*}{\kappa} \ln\left(\frac{z}{z_0}\right) \tag{1}$$

which can be rearranged into a slope-intercept form as follows:

$$\kappa \cdot u(\ln z) = u_* \cdot \ln z - u_* \cdot \ln z_0 \tag{2}$$

To evaluate the appropriateness of the semi-logarithmic fit to the wind speed data, a linear regression coefficient R^2 was computed for the linear function $u(ln\ z)$ for every 20-minute sample.

To adjust the results for the non-stationary wind speed and direction some form of normalization was required. This was accomplished in a third step by dividing each 20-minute average value of u_* by the analogous and synchronous value measured at Station 1, i.e. the reference station near the center or downwind edge of the lake. The normalized

values of u_* for each mobile station and Station 2 were averaged for the entire record length at each station.

The shear stress or shear velocity on the lake surface is expected to be a function of wind fetch. Fetch is the distance of a station from the edge of the lake measured in the upwind direction. The fetch was determined from GPS coordinates of each station and measurements taken from a USGS 7.5 minute quadrangle map. The fetch was measured for every station in 30º increments of direction around the lake perimeter. The fetch was computed from the edge of the reeds as well as from the trees surrounding the open lake surface, since either could be the dominant sheltering element. As the wind direction changed, the fetch changed as a function of wind direction. Like the shear velocity data, fetch was calculated as an average for time windows of 20 minutes. The multiple fetch values were averaged over the measurement day for each station, and represented graphically as a single point average, with error bars representing one standard deviation of the basic 2-minute or 10-second data set.

5. Field Results for Round Lake 2004

We first determined an integral time scale of the cup anemometer velocity data by autocorrelation analysis. Examples of autocorrelograms of the wind speed and wind direction data from 03-Mar-2004 are shown in Figure 5. The integral time scale was defined as the lag time at which the autocorrelation coefficient reached a value of 1/e (≈ 0.37). The autocorrelation coefficient had approximately the same value for the three elevations (from 0.3 to 2.5m above the lake surface?) at which wind speeds were measured (Table 1). The value of the integral time scale determined in this way was approximately 3 minutes. Averaging of measured wind velocities over 20-minute sampling periods was therefore deemed appropriate.

The results of the shear velocity computations are presented in Figures 2(a) to 2(d) along with maps, showing station locations and mean wind direction. Average values of u_* over the record length are plotted; the variation in u_* throughout the record length is indicated by an error bar which represents one standard deviation about the mean. Normalized shear velocities are plotted against fetch in Figures 2(a) to 2(d). Like the shear velocity data, the multiple fetch values are averaged over the period of measurement for each station, and represented as a single point in Figures 2(a) to 2(d) with error bars indicating one standard deviation about the mean.

Figures 2(a) and 2(b) suggest that shear velocities (stresses) on the lake vary the most over the first 500m downwind of the transition from land (vegetation and residential structures) to the lake, and that the shear stress at the transition point is at least an order of magnitude smaller than that measured far downwind.

To evaluate the appropriateness of the semi-logarithmic $u(ln\ z)$ fit to the wind speeds recorded at three elevations above the lake surface, a linear regression coefficient R^2 was computed for each of the 20-minute averaging intervals at each station. In general, the regression analysis revealed that the linear fit of the *u(ln z)* plot was better for the

downwind stations than the upwind stations (Figure 6a). Occasional deviations occurred in time, but were seemingly not dependent on wind direction (Figure 6b).

Figure 6b gives the regression coefficients for the 20-minute average wind speed data for Stations 1 and 2 on 03-Mar-2004. Station 1 is near the center of the lake, and Station 2 is near the upwind edge (Figure 2(a)).. The regression coefficient R^2 for both stations is generally greater than 0.99, but there are more excursions into lower R2-values at Station 2, i.e. near the upwind edge of the lake. One period of anomalously low correlation occurred between 250 and 300 minutes. The wind direction is plotted to demonstrate that this anomaly is not related to a shift in wind direction. The period of low correlation corresponds to a period of relatively quiescent wind during which the wind speed was at least 20-50% lower than its average over the entire period of measurement. The minimum R^2, even during this period of "low" correlation is 0.92.

A high linear regression coefficient of the wind speed as a function of ln *z* suggests that the log profile is an appropriate fit to the 3-point measurements. Examples of the linearity associate with different regression coefficients R^2 are shown in Figure 7. These velocity profiles indicate noticeable deviation from a straight line, representative of the semi-log velocity profile, even for relatively high regression coefficients such as 0.92.

The sonic anemometers recorded high frequency (20 Hz) fluctuations of three orthogonal components of wind velocity from which Reynolds stress could be calculated. Figures 8(a) gives shear velocity obtained from one sensor at Station 2 at a height of 0.93m on 3 March 2004. Figures 8(b) and (c) give the shear velocity computed at two different locations on 12 March 2004. In all three plots the values of shear velocity are based on 5-minute averages as suggested by Vickers and Mahrt (1997) for sonic anemometer data. The shear velocity computed from the associated cup-anemometer data (12-minute averages) is shown for comparison in all three plots. The value of the shear velocity u* computed from the Reynolds stress is about twice that computed from the slope of the velocity profile. We will discuss this large difference in the next section.

6. Discussion

To enhance our interpretation and understanding of the field observations we need to consider the transition from the land and vegetation to the flat and open lake surface. The change in the velocity profiles in the transition region can be related to the adjustment and growth of several boundary layers (Figure 9). The area pictured in Figure 9 may be about 50m high and 1000m long. Coming from the land with reeds or trees on it, we would expect to have a velocity profile typical of a plant canopy (Garratt 1992) with a near-zero velocity at the penetration depth inside the canopy. As the wind encounters the lake surface, the zero-velocity plane is suddenly lowered. Whatever flow comes through the vegetation onto the lake has a small velocity, dependent on the 'permeability' or flow resistance of the vegetation. We will ignore that velocity. As the wind flow over the canopy encounters the stagnant air layer over the lake a ***'blending layer'*** begins to develop between those two layers (Figure 9). This blending layer grows in height (thickness) in the downstream direction until it reaches the lake surface. If the land surface up to the edge of the lake is covered by buildings a 'separation streamline' with a slope on the order of 1: n (n= 6 to 10) and a 'point of reattachment' where this separation streamline reaches the lake surface, have been introduced in previous studies (give references). The concept of a 'separation zone' ending at the 'point of reattachment' looses its validity for a vegetated area, especially if its 'permeability' is high, i.e. its resistance to wind flow is low. At best a separation region can exist only between the penetration depth in the canopy and the lake surface.

At the same time as the blending layer develops in downwind direction, the presence of the lake surface is felt by the wind coming off the land, resulting in the development of an ***'internal boundary layer'*** of increasing thickness in windward direction. While this boundary layer is in principle similar to the classical flat plate boundary layer, it also has several substantial differences:

(1) There is no well defined free stream velocity at x=0, i.e. the beginning of the lake surface. In a separation zone, as described above, the wind velocity on the lake surface

could even be negative up to the re-attachment point. With an on-land vegetation cover, there may be a small positive wind velocity at the beginning of the lake. The shear stress on the water surface on the upwind edge of the lake will be small relative to a downwind value of shear stress, and far from the infinite value at the leading edge of a flat plate.

(2) The boundary layer growth of the boundary layer on a flat plate is solely controlled by the plate's surface roughness and the free stream velocity. The aerodynamic roughness of a lake surface, i.e. an ice and snow cover in winter or a water surface in summer is more or less known. However, above a lake there is no constant free stream velocity. Instead the velocity above the interior boundary layer changes in downwind direction from the velocity that comes out of the upwind vegetation cover to the velocity in the blending layer, and further downstream to the velocity in the 500m to 1000m thick atmospheric boundary layer. That makes the boundary layer growth harder to specify.

(3) The shear stress on a flat plate diminishes with distance from the leading edge, while the shear stress on a lake surface is likely to increase with distance from the lake's edge, a substantial difference!

A third boundary layer, thinner than the interior boundary layer, is identified as the ***'equilibrium layer'*** in Figure 9. By definition, the surface shear stress, the turbulence, and the velocity profile in that layer are in equilibrium or uniquely related to each other. This layer can be described by the classical boundary layer relationships. It also grows in thickness in downwind direction.

In light of the above discussion we have to ask how the elevations z above the lake surface of the anemometers described earlier relate to this picture of multiple boundary and blending layers in the transition region from the land to the lake. Only measurements in the equilibrium layer (and with some stretch of the imagination in the internal boundary layer) should fit the classical semi-logarithmic law of the velocity profile. A poor linear regression fit (low R^2) as shown in Figure 7 may therefore indicate that the topmost anemometer was above the boundary layer. In that case the shear velocity representative of

the lake surface should be calculated only from the wind speed measurements at the two lowest elevations, not from all three. Computations of shear velocities were therefore repeated with data from only the two lowest anemometers. For a comparison, the shear velocities u_* obtained using both the three-point and the lower two-point fits for Station 1 in the middle of the lake and Station 2 at the upwind edge of the lake are shown in Figure 10. The shear velocity at the upwind station is smaller than in the middle of the lake as to be expected. To increase the accuracy of the results the shear velocities u_* plotted in Figure 2 are therefore those computed using the lower two anemometers only.

Using Figure 9 as a guide we can also attempt to explain the difference in shear velocities obtained from the cup anemometer data and the sonic anemometer data (Figures 8a to 8c). The shear stress in the turbulent boundary layer above the lake surface is the Reynolds stress. The sonic anemometer measures the turbulent velocity components u' and v' directly and calculates the Reynolds stress as the time-averaged value $\rho u'v'$. The cup anemometers measure mean wind velocities, not turbulent components; Reynolds stress has to be estimated by making the assumptions of the classical mixing length theory, i.e. the shear stress in the air boundary layer above the lake is constant and equal to the shear stress on the lake surface; turbulent velocity components are proportional to the mean velocity gradient with height, and mixing length is proportional to distance above the lake surface. In essence mixing length theory is build on the assumption that turbulence in the boundary layer is controlled entirely 'from the bottom up', i.e. from the lake surface. Turbulence imported from the blending layer above is entirely ignored. In the transition region from land to water this is probably not true. Turbulence imported from above is picked up by the sonic anemometer, but not by the cup-type anemometers. That may be the reason why the latter give a lower shear stress.

To further explore the boundary layer transition region from the land to a lake, additional wind velocity data were collected in the winter of 2004/2005 with anemometer arrays of five sensors at each station, and a sonic anemometer. These data have a higher vertical resolution. The procedures were similar to those in the winter of 2003/2004. However, the distance between anemometer arrays was extended by placing one fixed

station in the middle (ML) and in the farfield (FF) at about 900m from the upwind edge of the lake. The measurement stations are shown on the maps of Figures 11(a) to 11(d). Synchronously measured average velocity profiles are plotted at semi-log scale in Figure 12. Data from the farthest downwind station (FF) give the most linear semi-log plot as to be expected. Regression coefficients for this station range from 0.9 to 1.

To see the progressive spatial evolution of the velocity profiles in downwind direction we have plotted the velocity profiles from all stations (Figure 13). They were not measured synchronously, but are normalized relative to the velocity at the midlake station ML, to remedy that deficiency at least partially. The growth of the blending layer and of the interior boundary layer can be seen in the figure.

Average shear velocities were calculated from the gradient of average velocities measured synchronously at two elevations. The calculated shear stresses, normalized with reference to the shear stress at the lowest elevation of the mid-lake station ML are plotted against elevation above the water surface in Figure 14. The averaging periods are typically 30 minutes, except in for Stations 1 (about 50m fetch) and Stations 6 (about 300m) fetch.

The Stations 1 to 6 which are between 50m and 300m from the upwind edge of the lake show the greatest variation in shear stress. We must keep in mind, however, that we may have calculated these shear stresses making the erroneous assumption of a fully developed turbulent velocity profile over the total height of measurements. To be on the safe side, we consider only the lowest two anemometers to calculate the shear stress on the lake surface. The resulting normalized shear velocity vs. fetch plot is given in Figures 11(a) to 11(x). The plots should be similar to Figures 2(a) and 2(b).

7. Conclusions

Not surprisingly, the velocity at the lake surface tends to increase with fetch. Likewise, the shear velocity (shear stress) increases with fetch. This is markedly different than the shear stress evolution along a flat plate, wherein the shear stress tends to be highest at the leading edge, and diminishes downwind. Based on the results of our work, it is difficult to quantify and describe exactly the physics of the flow after these transitions at all potential ranges of wind speed. A few useful generalizations, however, can be stated with confidence for "normal" wind conditions observed at lakes with perimeter vegetation similar to that at our field sites.

First, for transitions of thick forest canopies to smooth water or ice surfaces in areas of flat topography, the shear stress approaches zero at the leading edge of the water or ice surface. The exact value of the normalized u* at this leading edge is a complicated function of the wind structure and upwind conditions, but for a reasonably thick canopy, the value of normalized u* will generally be small (and the value of the corresponding normalized shear stress will be smaller yet since it is a function of the square of u*). The value of the normalized u* increases from the leading edge to an approximately maximum value at a fetch of about 50 canopy heights (400-500m). Beyond this fetch, we didn't observe significant increases in the value of u*. This is interpreted to indicate that the equilibrium layer and/or the canopy-top blending layer extend throughout the range of measurement elevations.

Second, for transitions between forest and lake that have a substantial fetch of intermediary reeds and marsh grasses, the interpretation is less straightforward. Some confusion arises regarding the proper way to measure fetch – should the measurement be made from the tree-line or the reed-line? The figures displayed in this paper use fetch measurements from the tree-line. The plots of normalized u* vs. fetch, when extrapolated back to zero fetch, would seem to indicate a baseline value of normalized u* of approximately 0.5. Given the results of direct forest-lake transitions – i.e. the baseline value of normalized u* is zero – this result is somewhat counterintuitive. For practical purposes

like lake hydrodynamic modeling, however, these generalized observations of the behavior of normalized u* downwind of reeds represent sufficient progress.

Third, on lakes where the sheltering is controlled by topography, the result is very similar to that where the sheltering is characterized by an abrupt transition of trees to water or ice – the upwind value of normalized u* approaches zero and increases downwind to some quasi-asymptotic value. In the case described herein, it appears that the fetch value at which normalized u* reaches its maximum value is larger than it was for the tree-sheltered lake, perhaps 10^3m. For fetches measured in canopy-height units, however, there may be no difference. More work is required to determine a proper sheltering model for topographically sheltered lakes.

References

Anderson RY, Dean WE. 1988. Lacustrine varve formation through time. *Palaeogrogr. Palaeoclimat. Palaeoecol. 62: 215-235*

Anis A, Moum JN. 1995. Surface wave-turbulence interactions – scaling e(z) near the sea-surface. *J. Phys. Oceanogr. 25: 2025-45*

Banner ML, Peregrine DH. 1993. Wave breaking in deep water. *Annu. Rev. Fluid Mech. 25: 373-97*

Banner ML, Phillips OM. 1974. On the incipient breaking of small scale waves. *J. Fluid. Mech. 65: 647-56*

Bäuerle E. 2001. Three-dimensional wind-induced baroclinic circulation in rectangular basins. *Adv. Water Res. 24: 11-27*

Bear J. 1988. Dynamics of fluids in porous media. *Dover Pubns. 784 pp.*

Belcher SE, Hunt JCR. 1998. Turbulent flow over hills and waves. *Annu. Rev. Fluid Mech. 30: 507-38*

Bicudo JR. 1988. The measurement of reaeration in streams. *PhD Dissertation. University of Newcastle upon Tyne. 383 pp.*

Bicudo JR, Giorgetti MF. 1990. The effect of strip bed roughness on the reaeration rate coefficient. *Proceedings of the 15th Biennial International Conference of the IAWPRC. Kyoto, Japan.*

Bradley E, Coppin P, Godfrey J. 1991.Measurements of sensible and latent heat flux in the western equatorial Pacific Ocean. *J. Geophys. Res. 96:3375-89*

Burchard H. 2001. Simulating the wave-enhanced layer under breaking surface waves with two equation turbulence models. *J. Phys. Oceanogr. 31: 3133-45*

Charnock H, 1955. Wind stress on a water surface. *Q.J.R. Meteorol. Soc. 350:639-40*

Condie SA, Webster IT. 2001. Estimating stratification in shallow water bodies from mean meteorological conditions. *J. Hydraulic Eng. 127(4): 286-92*

Dake JMK, Harleman DRF. 1969. Thermal stratification in lakes: analytical and laboratory studies. *Water Res. Res. 5(2): 484-495*

Danckwerts PV. 1951. Significance of liquid-film coefficients in gas-absorption. Introduction of the surface renewal concept. *Ind. Eng. Chem.* 43(6): 1460-1467

Dorman CE, Mollo-Christensen E. 1973. Observation of the structure of moving gust patterns over a water surface. *J. Phys. Oceanogr. 3: 120-32*

Edinger JE. 2001. Waterbody hydrodynamic and water quality modeling: An introductory workbook and CD-ROM on three-dimensional waterbody modeling. *ASCE Press. 215 pp.*

Fairall CW, Bradley EF, Rogers DP, Edson JB, and Young GS. 1996. Bulk parameterization of the air-sea fluxes for Tropical Ocean-Global Atmosphere Response Experiment. *J. Geophys. Res. 101: 3747-64*

Farell C, Iyengar AKS. 1999. Experiments on the wind tunnel simulation of atmospheric boundary layers. *J. of Wind Engin. 79: 11-35*

Finnegan J. 2000. Turbulence in plant canopies. *Annu. Rev. Fluid Mech. 32: 519-571*

Garrett JR, 1992. *The atmospheric boundary layer*. Cambridge University Press, Cambridge UK, 316 pp.

Geernaert GL, Davidson K, Larsen S, Mikkelsen T. 1988. Wind stress measurements during the tower ocean wave and radar dependence experiment. *J. Geophys.Res. 93: 13913-23*

Guan D, Zhang Y, Zhu T. 2003. A wind-tunnel study of windbreak drag. *Agric. For. Meteorol. 118: 75-84*

Haidvogel DB, Wilkin JL, Young R. 1991. A semi-spectral primitive equation ocean circulation model using vertical sigma and orthogonal curvilinear horizontal coordinates. *J. Comp. Phys. 94: 151-*

Higbie R. 1935 Penetration theory leads to use of the contact time in the calculation of the mass transfer coefficients in the two film theory. *Trans. Am. Inst. Chem. Engrs 31: 365*

Hocking GC, Patterson JC. 1994. Modelling tracer dispersal and residence time in a reservoir. *Ecol. Model. 74(1-2): 63-75*

Hondzo M, Stefan HG. 1993. lake water temperature simulation model. *J. Hydraulic Eng. ASCE 119(11):1251-1273*

Jähne B and Hauβecker H. 1998, Air-water gas exchange. *Annu. Rev. Fluid Mech. 30: 443-68*

Jessup AT, Zappa CJ, Yeh H. 1997. Defining and quantifying microscale wave breaking with infrared imagery. *J. Geophys. Res. 102(C10): 23,145-53*

Kenney WA. 1987. A method for estimating windbreak porosity using digitized photographic silhouettes. *Agric. For. Meteorol. 39: 91-94*

Kolb BH, Heineman MC. 1995. Controlling mechanisms of sediment-driven dissolved oxygen dynamics in New Bedford Outer Harbor. *Marine Freshwater Res. 46(1): 69-79*

Lawrence I, Breen P. 1998. Design guidelines: stormwater pollution control ponds and wetlands. *CRCFE Rep.* Cooperative Research Centre for Freshwater Ecology, Canberra, Australia

Mastenbroek K. 1998. High-resolution wind fields from ERS SAR. *Earth Obs. Quart. 59: 20-22*

Melville WK. 1996. The role of surface-wave breaking in air-sea interaction. *Annu. Rev. Fluid Mech. 28: 279-321*

Mourad PD, Walter BA. 1996. Viewing a cold air outbreak using satellite-based synthetic aperture radar and advanced very high resolution radiometer imagery. *J. Geophys. Res. 101 (C7): 16,391-400*

Mourad PD, Thompson DR, Vandemark DC. 2000. Extracting fine-scale wind fields from synthetic aperture radar images of the ocean surface. *Johns Hopkins APL Tech. Dig. 21(1): 108-115*

Porté-Agel F, Meneveau C, Parlange MB. 2000. A scale dependent dynamic model for large-eddy simulation: application to a neutral atmospheric boundary layer. *J. Fluid Mech. 415:261-84*

Porté-Agel F, Parlange MB, Meneveau C, Eichinger W. 2001. A priori field study of the subgrid-scale heat flux and dissipation in the atmospheric surface layer. *J. Atmos. Sci. 58: 2673-98*

Porté-Agel F, Pahlow M, Meneveau C, Parlange MB. 2001. Atmospheric stability effect on subgrid-scale physics for large-eddy simulation. *Adv. Water Res. 24(9-10):1085-102*

Portielje R, Lijklema L. 1995. The effect of reaeration and benthic algae on the oxygen balance of an artificial ditch. *Ecol. Model. 79(1): 35-48*

Schlichting H, Gersten K. 2000. *Boundary layer theory. 8th revised and enlarged edition.* Springer. 799 pp.

Schulz HE. 1990. Investigation of the flowing water reoxygenation mechanism and its correlation with the turbulence level near the surface – II. *PhD Dissertation. University of São Paulo, Brazil (In Portugese)*

Schulz HE, Bicudo JR, Barbosa AR, Giorgetti MF. 1990. Turbulent water aeration: analytical approach and experimental data. In *Air Water Mass Transfer. Eds. Wilhelms SC, Gulliver JS. ASCE Press. 142-155*

Scully NM, Leavitt PR, Carpenter SR. 2000. Century-long effects of forest harvest on the physical structure and autotrophic community of a small temperate lake. *Can. J. Fish. Aquat. Sci. 57(Suppl. 2): 50-59*

Sikora TD, Thompson DR, Bleidorn, JC. 2000. Testing the diagnosis of marine atmospheric boundary layer structure from synthetic aperture radar. *Johns Hopkins APL Tech. Dig. 21(1): 94-99*

Simon A, Kocsis O, Stips A, Wüest A. 2002. Momentum and turbulent kinetic energy balance in the surface boundary layer of developing waves. *J. Geophys. Res. (no pub date yet)*

Smagorinsky JS. 1963. General circulation experiments with the primitive equations: 1. the basic experiment.*Mon. Weather Rev. 91: 99-164*

Smits, AJ. 2000. A physical introduction to fluid mechanics. *John Wiley & Sons. 527 pp.*

Steedman RJ, Kushneriuk RS. 2000. Effects of experimental clearcut logging on thermal stratification, dissolved oxygen, and lake trout (*Salvelinus namaycush*) habitat volume in three small boreal forest lakes. *Can. J. Fish. Aquat. Sci. 57(Suppl. 2): 82-91*

Stoffelen A, Anderson DLT. 1993. Wind retrieval and ERS-1 scatterometer radar backscatter measurements. *Adv. Space. Res. 13: 53-60*

Stull RB. 1988. An introduction to boundary layer meteorology. *Kluwer Acad. Publ. 670 pp.*

Terray EA, Donelan MA, Agrawal YC, Drennan WL, Kahma KK, et al. 1996. Estimates of kinetic energy dissipation under breaking waves. *J. Phys. Oceanogr.26: 792-807*

Thitimajshima P, Rangsanseri Y, and Rakprathanporn P. 1998. A simple SAR speckle reduction by wavelet thresholding. *Proc. 19th Asian Conference on Remote Sensing (ACRS).*

Thompson DR, Beal RC. 2000. Mapping high-resolution wind fields using synthetic aperture radar. *Johns Hopkins APL Tech. Dig. 21(1): 58-67*

Thorpe SA. 1995. Dynamical processes of transfer at the sea surface. *Prog. Oceanogr. 35: 315-52*

Upstill-Goddard RC, Watson AJ, Liss PS, Liddicoat, MI. 1990. Gas transfer in lakes measured with SF_6. Tellus B.: 42(4): 364-377

Van Dorn W. 1953. Wind stress on an artificial pond. *J. Marine Res. 12: 249-276*

Vicjers D, Mahrt L. 1997. Quality control and flux sampling problems for tower and aircraft data. *J. Atm. Oc. Tech.* 14: 512-526

Wang H, Takle ES, Shen J. 2001. Shelterbelts and windbreaks: mathematical modeling and computer simulations of turbulent flows. *Annu. Rev. Fluid Mech. 33: 549-86*

Wang Y, Hutter K. 1998. A semi-implicit semispectral primitive equation model for lake circulation dynamics and its stability performance. *J. Comp. Phys. 139: 209-41*

Wang Y, Hutter K, Bäuerle E. 2001. Three-dimensional wind-induced baroclinic circulation in rectangular basins. *Adv. Water Res. 24: 11-27*

*W*ang Y. 2003. Importance of subgrid-scale parameterization in numerical simulations of lake circulation. *Adv. Water Res. 26: 277-94*

Wanninkhof R, Ledwell J, Crusius J. 1990. Gas transfer velocities on lakes measured with sulfur hexafluoride. In: *Air Water Mass Transfer*. Eds.

Wanninkhof R, McGillis WR. 1999. A cubic relationship between air-sea CO_2 exchange and wind speed. *Geophys. Res. Lett. 26 (13): 1889-92*

Wilhelms, SC and Gulliver JS, ……American Society of Civil Engineers. 441-58

Wismann V. 1992. A C-band scatterometer model derived from the data obtained during the ERS-1 calibration/validation campaign. *Proc. First ERS-1 Symp., Cannes, France. 55-59*

Wu J. 1969. Wind stress and surface roughness. *J. Geophys. Res.74: 444-455*

Wu J. 1970. Wind-wave interactions. *Phys. Fluids. 13: 1926-1930*

Wüest A and Lorke A. 2003. Small-scale hydrodynamics in lakes. *Annu. Rev. Fluid Mech. 35: 373-412*

Yelland MJ, Taylor PK. 1996. Wind stress measurements from the open ocean. *J. Phys. Oceanogr. 26: 541-58*

Appendix A: Flat Plate Similarity Justification

To justify conducting wind experiments over the ice layer of a lake rather than the open water, we rely on established relationships for shear stress as a function of wind speed for flat solid surfaces (plates) and water surfaces. In either case, the kinematic shear stress τ/ρ is given by:

$$\frac{\tau}{\rho} = C_{D,h} U_h^2 \tag{A1}$$

where U_h is the wind speed measured at height h and $C_{D,h}$ is the drag coefficient corresponding to the wind speed measured at height h; in the case of the flat plate the value of U and C_D are based on the free stream values. For a flat plate under a free stream flow Schlichting and Gersten (2000) provide:

$$C_D = 2\left[\frac{\kappa}{\ln \mathrm{Re}_x} G(\ln \mathrm{Re}_x)\right] \tag{A2}$$

where the function $G(\ln \mathrm{Re_x})$ approaches a value of 1 at $\mathrm{Re_x} \rightarrow \infty$ and a value of ~1.3-1.4 for $\mathrm{Re_x} \sim 10^5$-10^6. In the present study, the range of $\mathrm{Re_x}$ is 10^7-10^8 for the entire range of reasonable fetches and wind speeds. The function G is, therefore, taken to be a constant with a value of 1.25. Von karman's constant κ is taken here to be equal to 0.4. Finally, for an open water surface, the drag coefficient is given by a variation of Charnock's equation (Charnock 1955, Wüest and Lorke 2003):

$$C_{D,h} = \left[\kappa^{-1} \ln\left(\frac{gh}{C_{D,h} U_h^2}\right) + 11.3\right]^{-2} \tag{A3}$$

Charnock's equation is valid for wind speeds greater than about 5 m/s. For lesser wind speeds – less than 3 m/s – the values of observed drag coefficients are yet to be adequately described by any physical model. Wüest and Lorke (2003) suggest the following empirical relationship for a wind speed measured at a height of 10 m:

$$C_{D,10} = 0.0044 U_{10}^{-1.15} \tag{A4}$$

Using equations 1-4, the wind shear stress on an ice cover (flat plate) can be compared to the wind shear stress on a water surface. The results are shown in Figure 2. For wind speeds up to 10 m/s, there is little discrepancy between the shear stress on a flat

plate and the shear stress on a water surface. It should be noted that Charnock's equation assumes a well developed wave field with a phase speed similar to the mean wind speed. For less developed wave fields, the frequency of wave formation and destruction is much greater, and requires a larger input of momentum for a given wind speed. Therefore, the values of shear stress plotted in Figure 2 ought to be taken as the lower bound on the shear stress that would be observed on a natural water surface.

Appendix B: Raw Data

02-21-2004

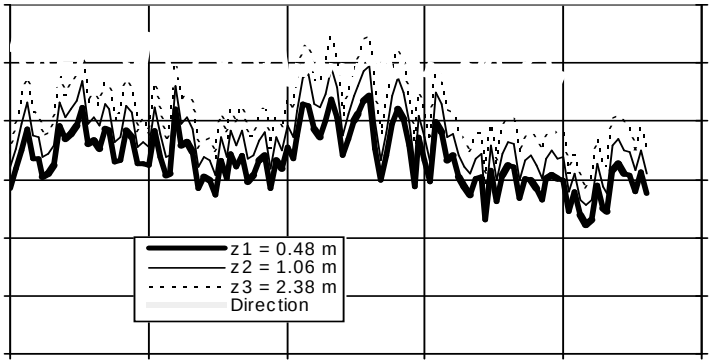

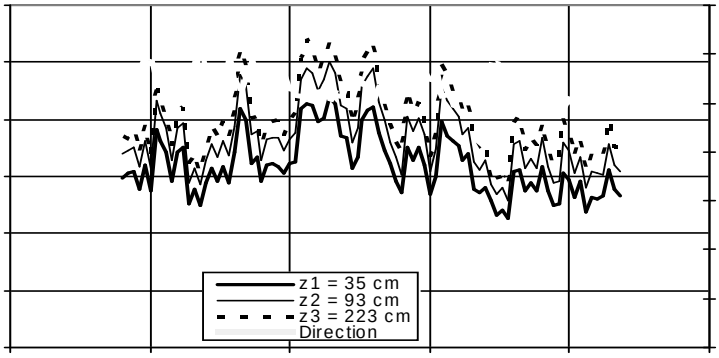

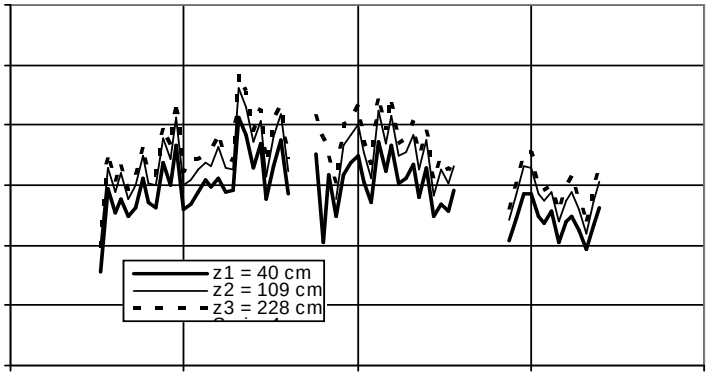

02-28-2004

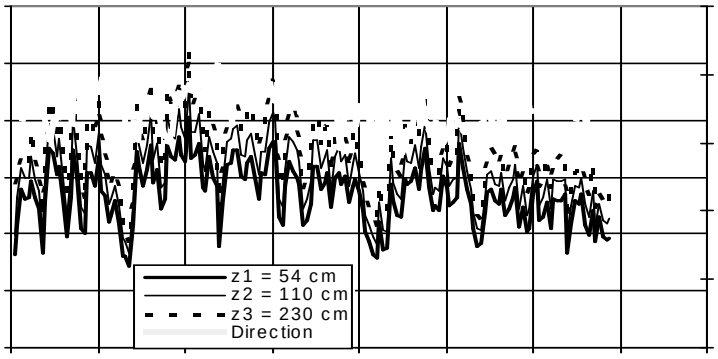
z1 = 54 cm
z2 = 110 cm
z3 = 230 cm
Direction

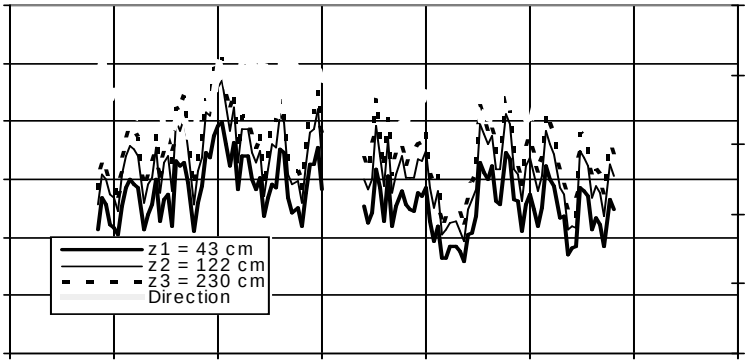
z1 = 43 cm
z2 = 122 cm
z3 = 230 cm
Direction

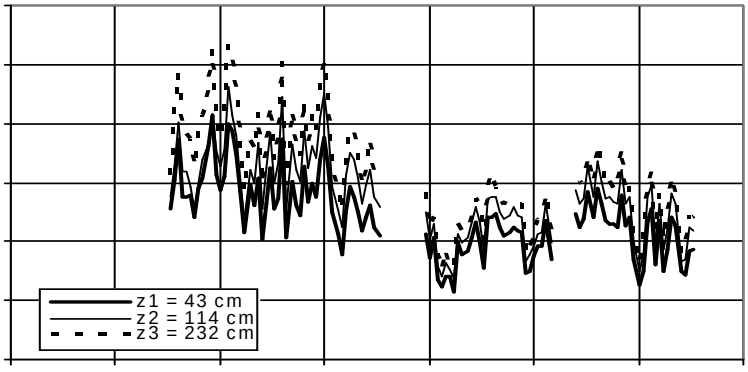
z1 = 43 cm
z2 = 114 cm
z3 = 232 cm

03-03-2004

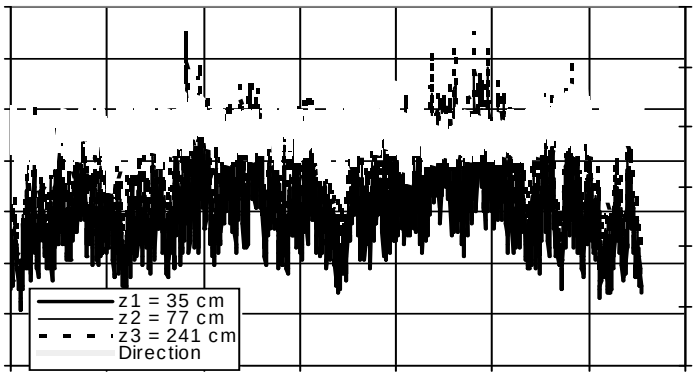
z1 = 35 cm
z2 = 77 cm
z3 = 241 cm
Direction

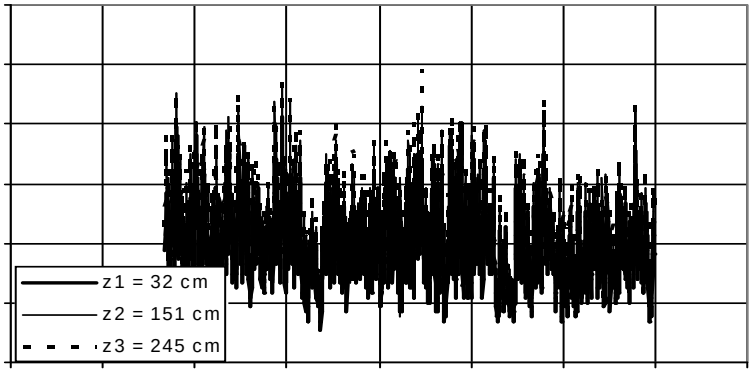
z1 = 32 cm
z2 = 151 cm
z3 = 245 cm

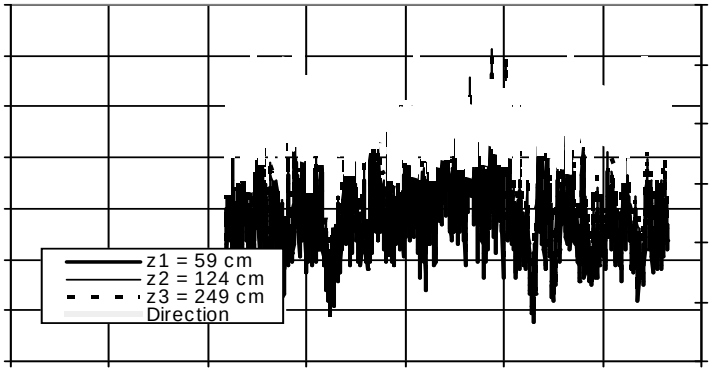
z1 = 59 cm
z2 = 124 cm
z3 = 249 cm
Direction

03-12-2004

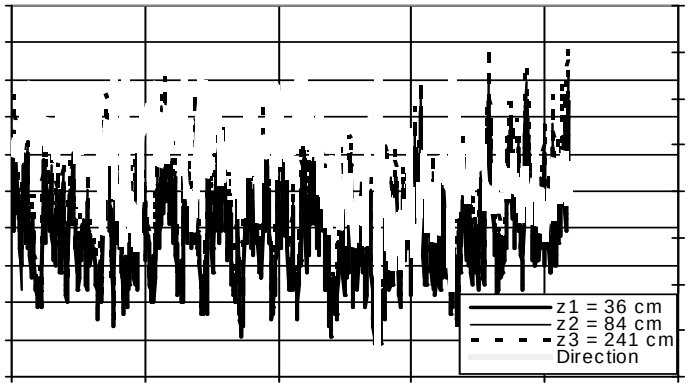
z1 = 36 cm
z2 = 84 cm
z3 = 241 cm
Direction

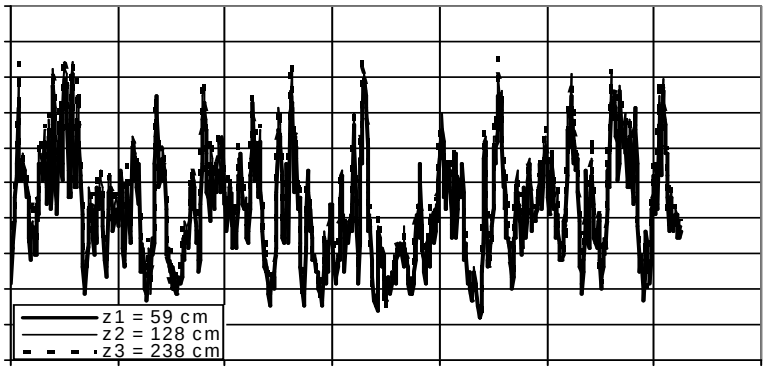
z1 = 59 cm
z2 = 128 cm
z3 = 238 cm

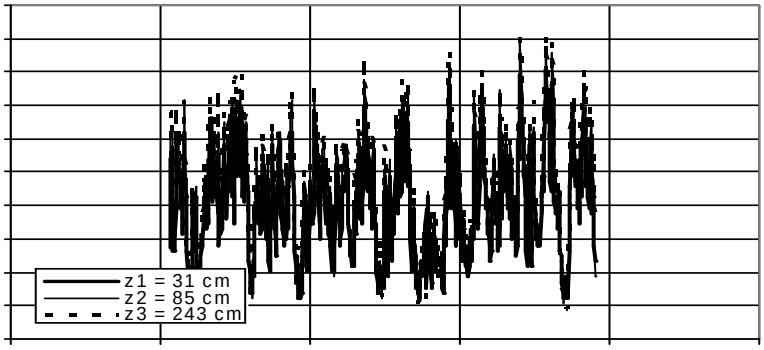
z1 = 31 cm
z2 = 85 cm
z3 = 243 cm

TABLES

Table 1: Instrument heights (m) above the lake surface for Round Lake 2004

Instrument	21-Feb-04	28-Feb-04	3-Mar-04	12-Mar-04
Station 1				
014A-1	0.5	0.5	0.4	0.4
014A-2	1.1	1.1	0.8	0.8
014A-3	2.4	2.3	2.4	2.4
direction	1.8	1.8	1.8	1.8
Station 2				
014A-1	0.4	0.4	0.3	0.6
014A-2	0.9	1.2	1.5	1.3
014A-3	2.2	2.3	2.5	2.4
direction	1.8	1.7	NA	NA
Mobile (Sta. 3)				
014A-1	0.4	0.4	0.6	0.3
014A-2	1.1	1.1	1.2	0.9
014A-3	2.3	2.3	2.5	2.4
direction	NA	NA	1.9	NA

Table 2: Instrument heights (m) above the lake surface for Lake Harriet 2005

Instrument	23 - Jan - 05
Station 1	Height (m)
014A-1	0.3
014A-2	0.7
014A-3	3.1
direction	2.3
Station 3	
014A-1	0.2
014A-2	0.7
014A-3	1.1
014A-4	3.1
direction	2.4
Mobile (Sta 2)	
014A-1	0.2
014A-2	0.5
014A-3	0.9
014A-4	1.3
014A-5	3.1
direction	NA

Table 3: Instrument heights (m) above the lake surface for Round Lake 2005

Instrument	5 Feb 2005	17 Feb 2005
Station 1		
014A-1	0.5	0.4
014A-2	0.8	0.8
014A-3	3.2	1.4
014A-4	NA	2.3
014A-5	NA	3.2
direction	2.5	2.7
Station 2		
014A-1	0.4	0.4
014A-2	0.7	0.7
014A-3	1.3	1.5
014A-4	3.2	2.2
014A-5	NA	3.2
direction	NA	2.7
Mobile		
014A-1	0.3	0.4
014A-2	0.7	0.8
014A-3	1.2	1.3
014A-4	1.9	2.2
014A-5	3.2	3.2
direction	NA	NA

FIGURES

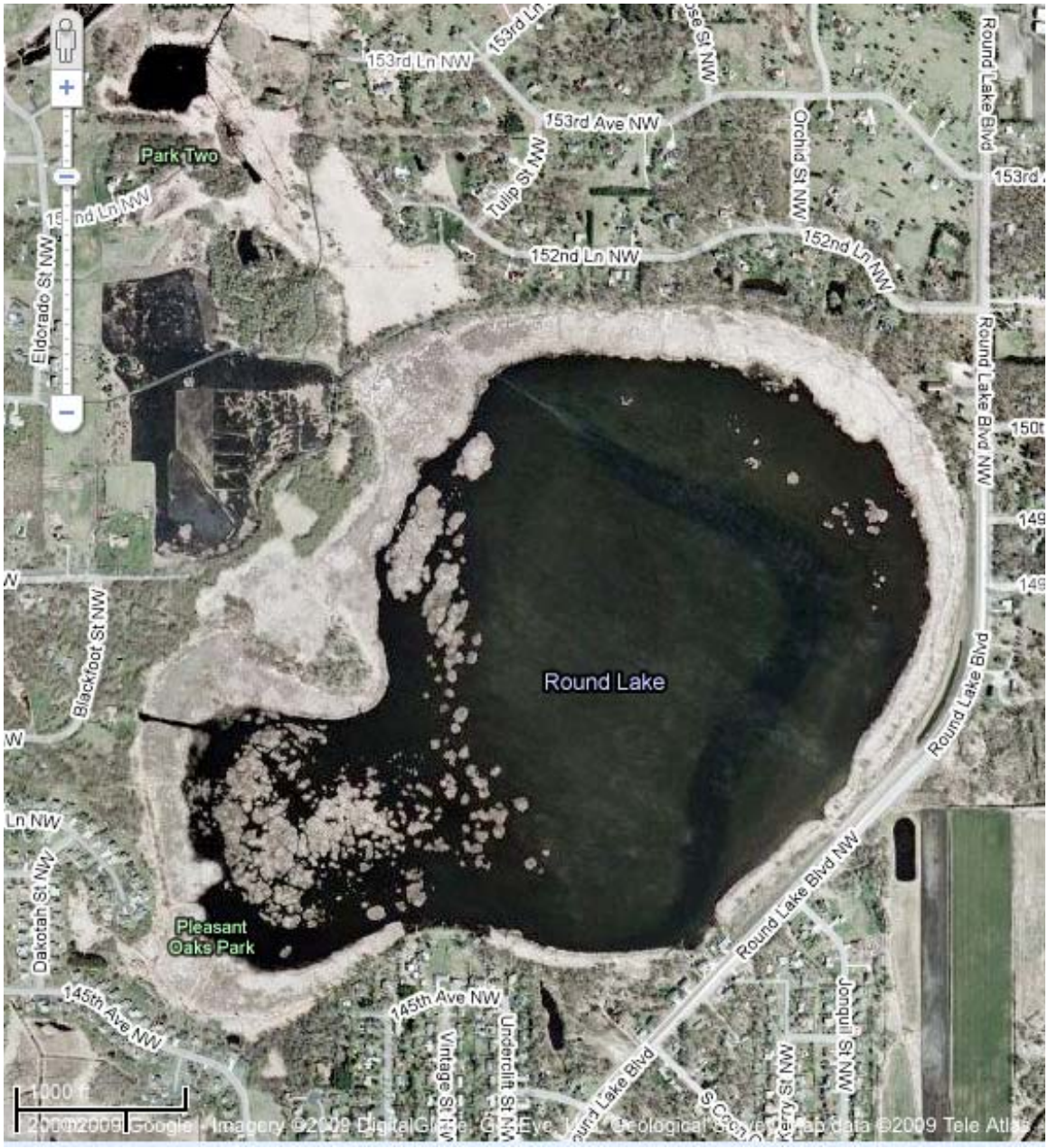

Figure 1. Round Lake field site. The local topography has low relief. The distance between the N-S trending red lines on the east- and the west-side of the lake is 1 mile (1.61 km). The lake surface area bounded by the reeds is approximately 1.1 km^2.

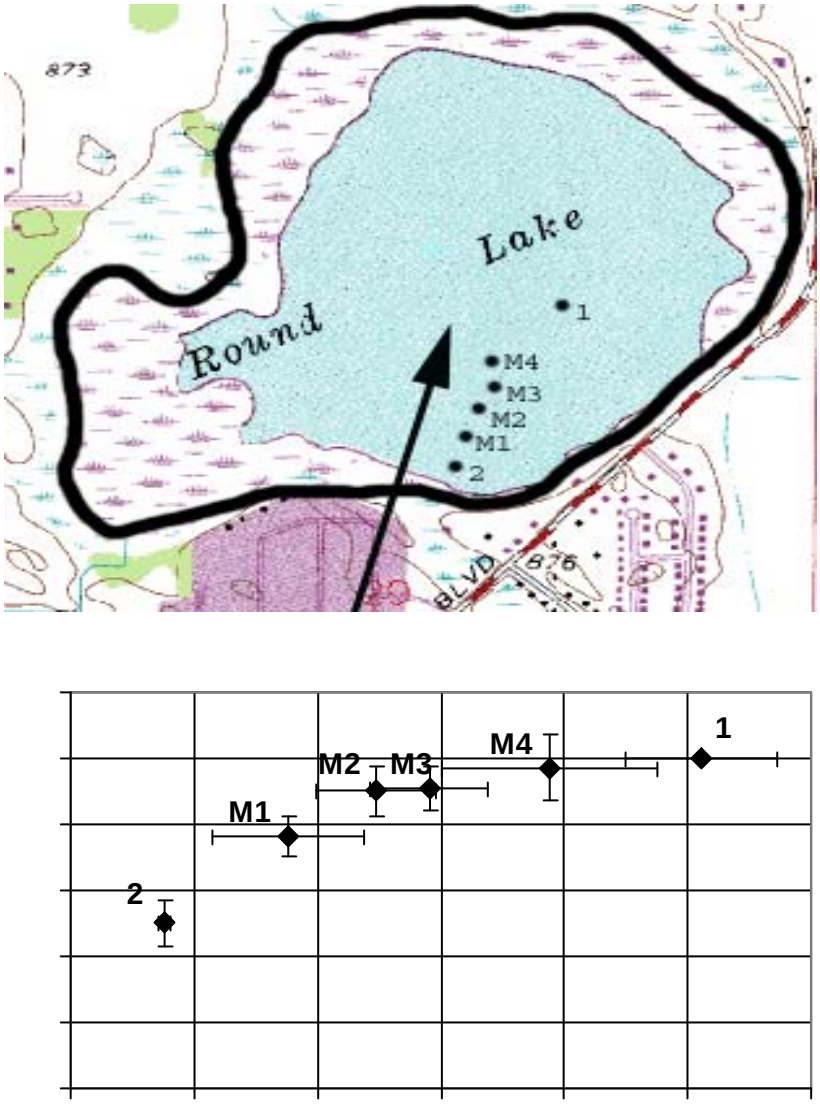

Figure 2a. (top) Station locations at Round Lake on 03 Mar 2004. Mobile stations are denoted by 'M'. The heavy black line denotes the boundary between land that is covered by reeds and that which is covered by trees. The E-W scale of the map is approximately 1 mile (1.6 km). Arrow indicates mean wind direction. (bottom) Normalized shear velocity as a function of fetch from trees, with error bars indicating 1 standard deviation.

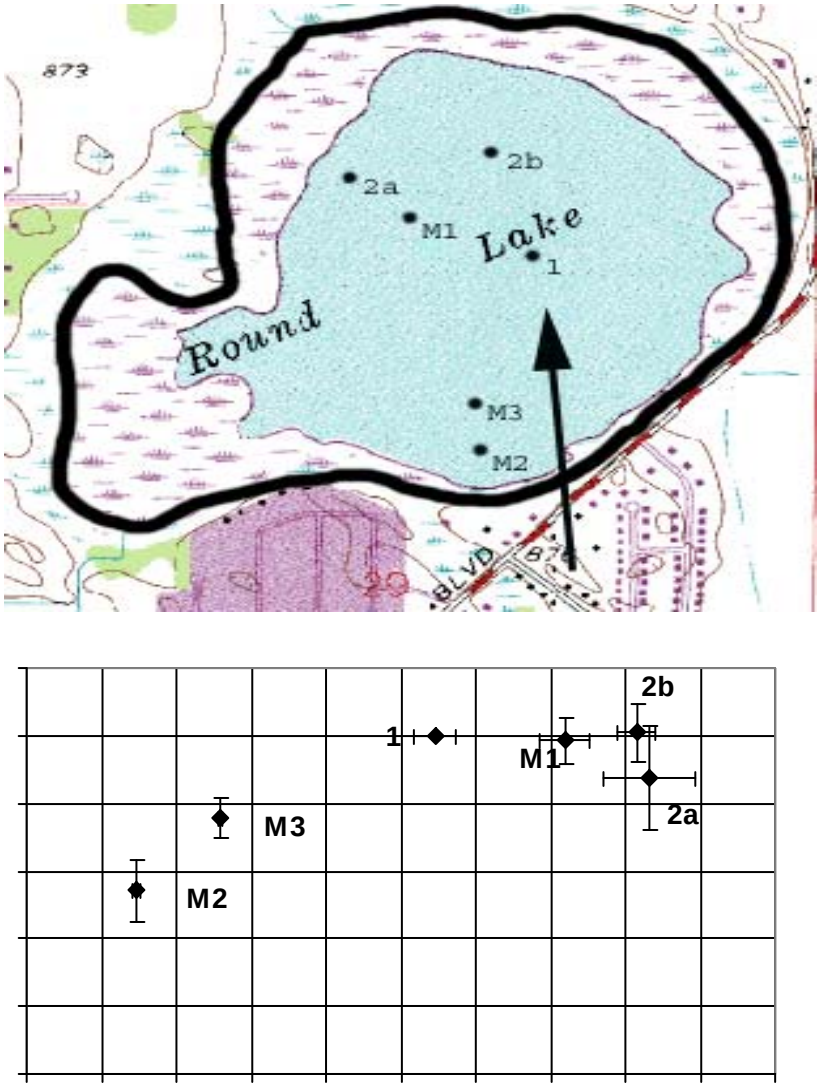

Figure 2b. (top) Station locations at Round Lake on 28 Feb 2004. Mobile stations are denoted by 'M'. Arrow indicates mean wind direction. (bottom) Normalized shear velocity as a function of fetch from trees, with error bars indicating 1 standard deviation.

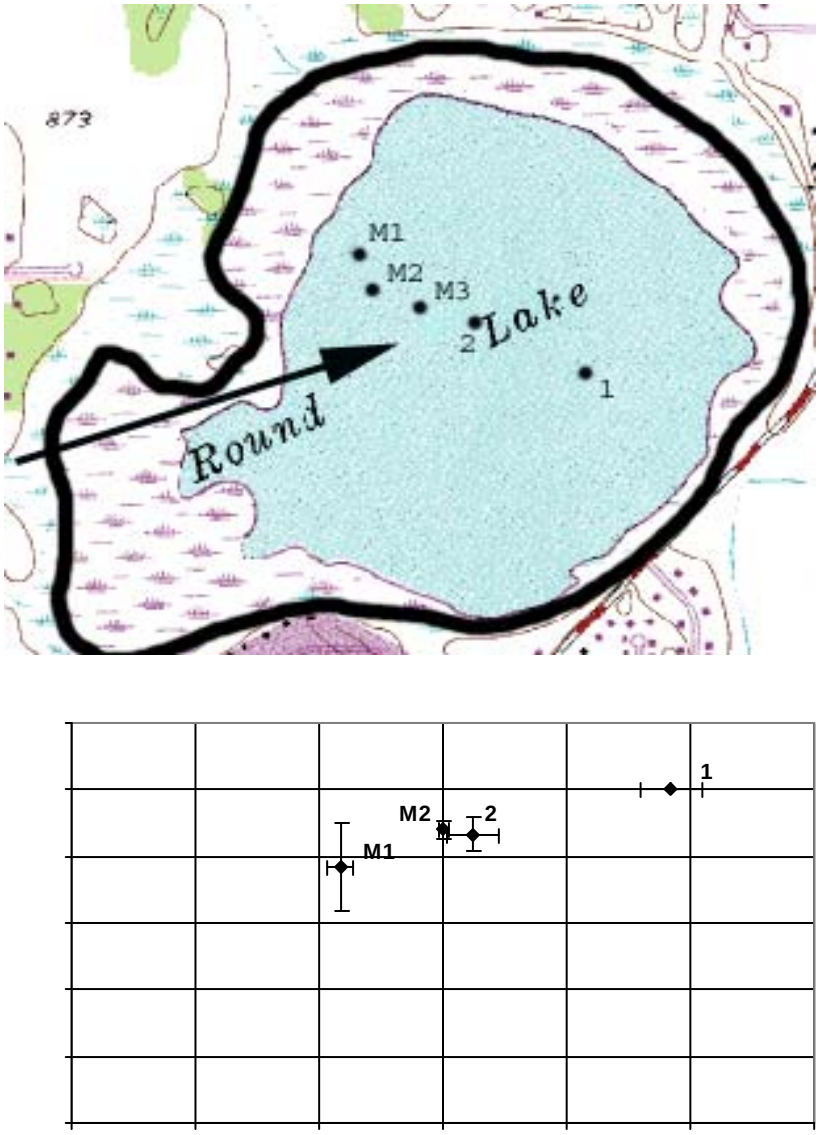

Figure 2c. (top) Station locations at Round Lake on 21 Feb 2004. Mobile stations are denoted by 'M'. Arrow indicates mean wind direction. (bottom) Normalized shear velocity as a function of fetch from trees perimeter, with all error bars indicating 1 standard deviation.

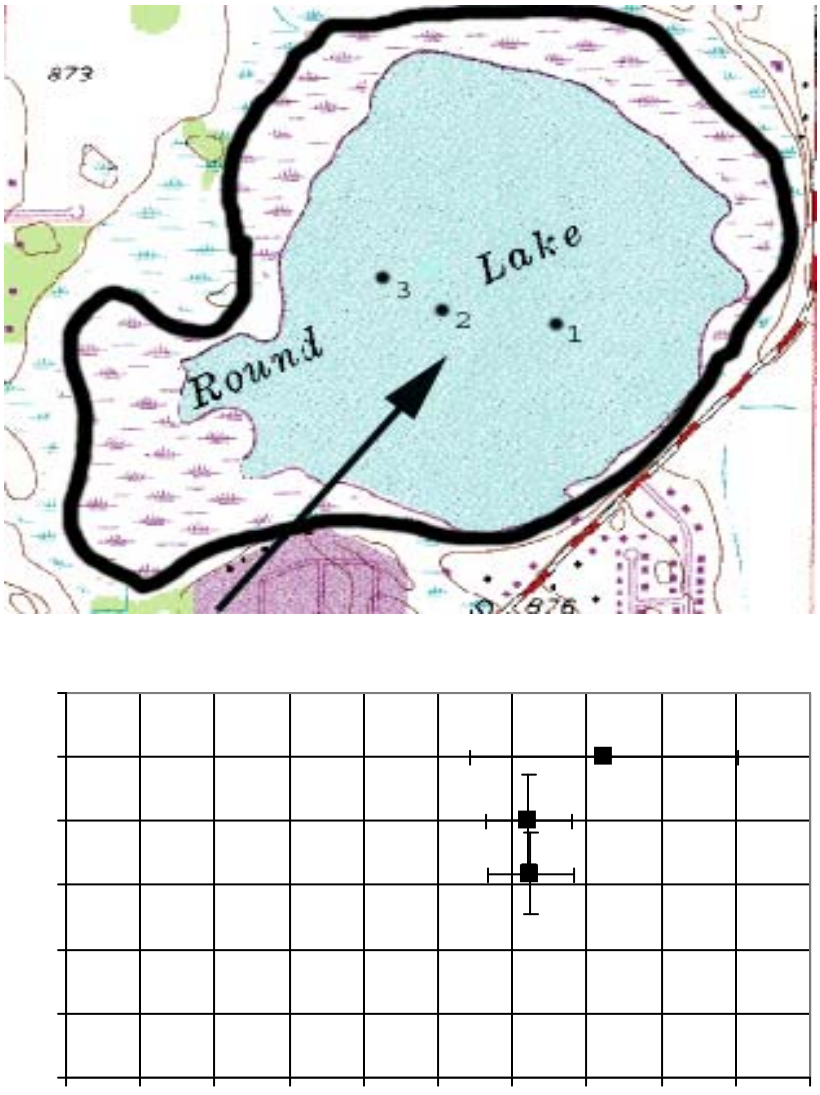

Figure 2d. (top) Station locations at Round Lake on 12 Mar 2004. Arrow indicates mean wind direction. (bottom) Normalized shear velocity as a function of fetch from trees and fetch from reeds, with error bars indicating 1 standard deviation.

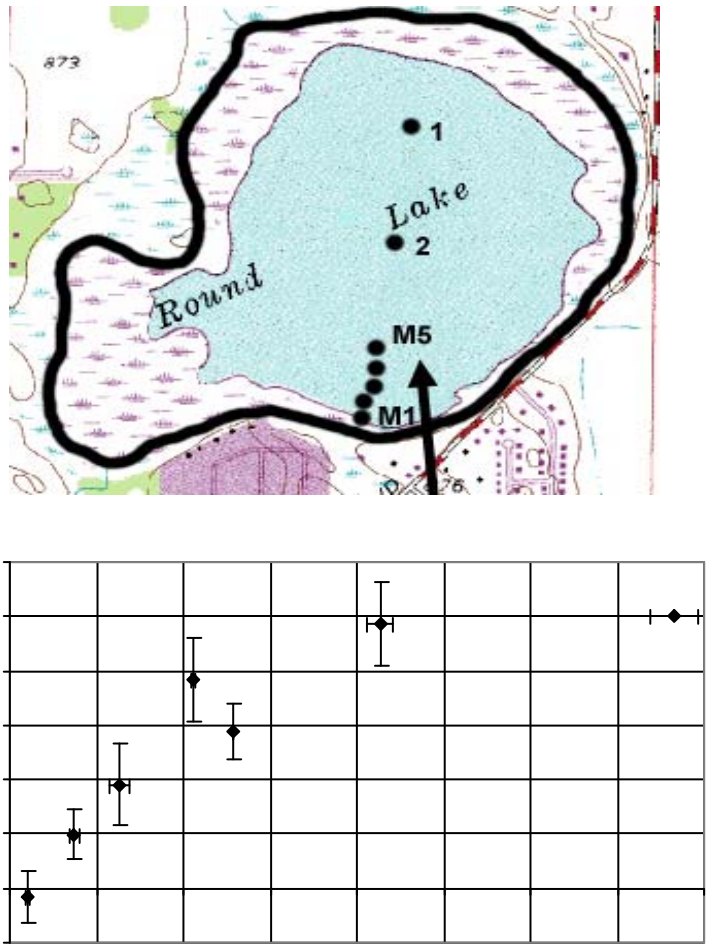

Figure 2e. (top) Station locations at Round Lake on 5 Feb 2005. Arrow indicates mean wind direction. (bottom) Normalized shear velocity as a function of fetch from trees, with error bars indicating 1 standard deviation.

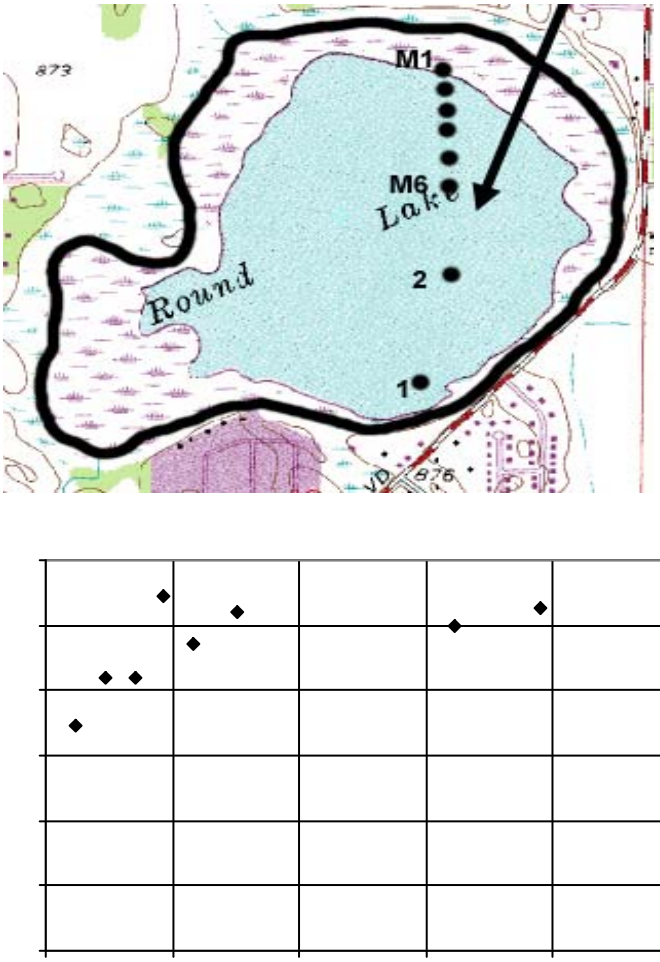

Figure 2f. (top) Station locations at Round Lake on 17 Feb 2005. Arrow indicates mean wind direction. (bottom) Normalized shear velocity as a function of fetch from trees, with error bars indicating 1 standard deviation. The situation here is different than that in previous plots in that the wind encounters reeds over a substantial distance after it crosses the shoreline/forest boundary.

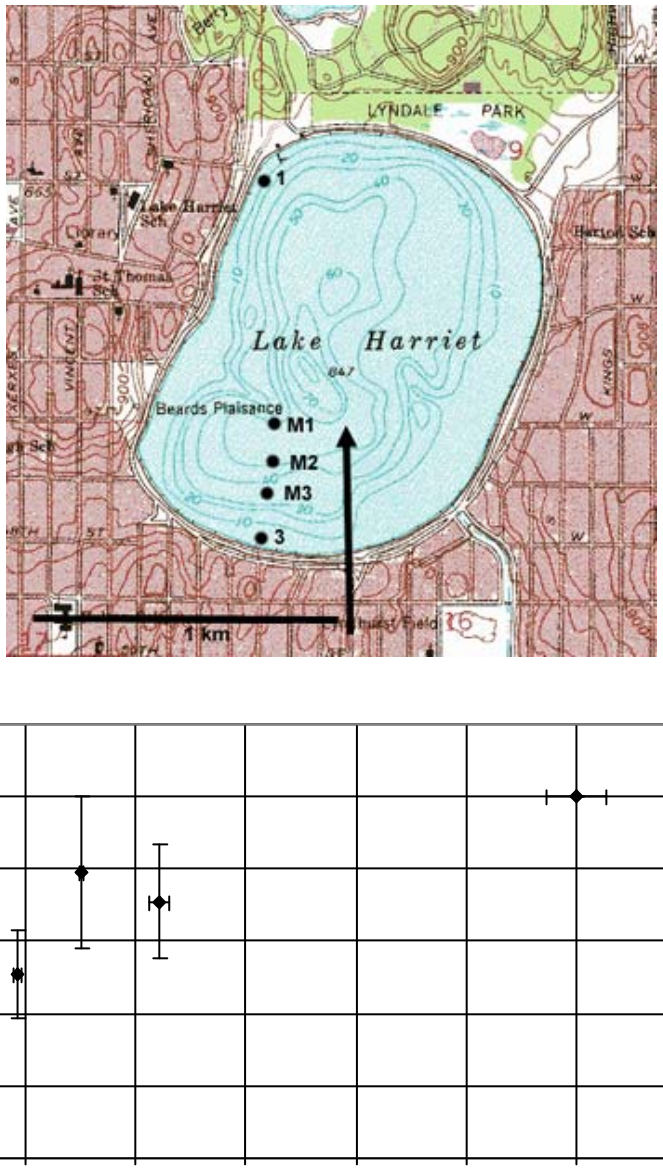

Figure 2g. (top) Station locations at Lake Harriet on 23 Jan 2005. Arrow indicates mean wind direction. (bottom) Normalized shear velocity as a function of fetch from trees, with error bars indicating 1 standard deviation.

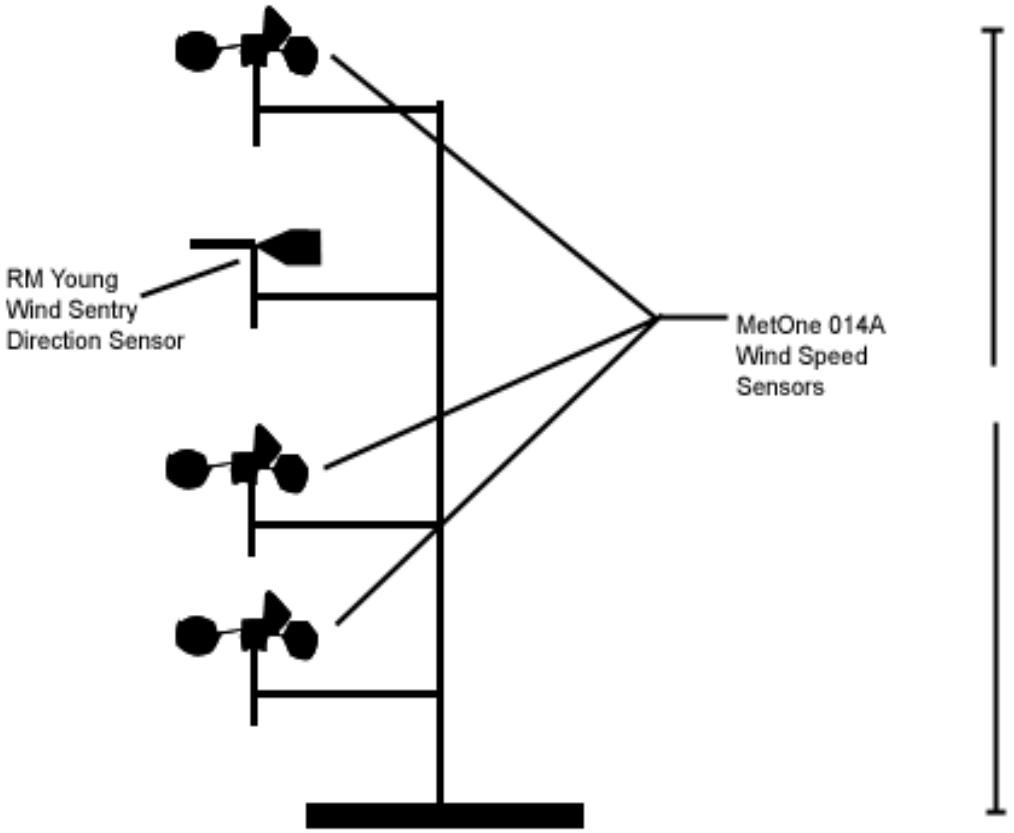

Figure 3: Sketch of the instrument set-up for the wind velocity profile measurement. Instrument heights are given in Tables 1-3.

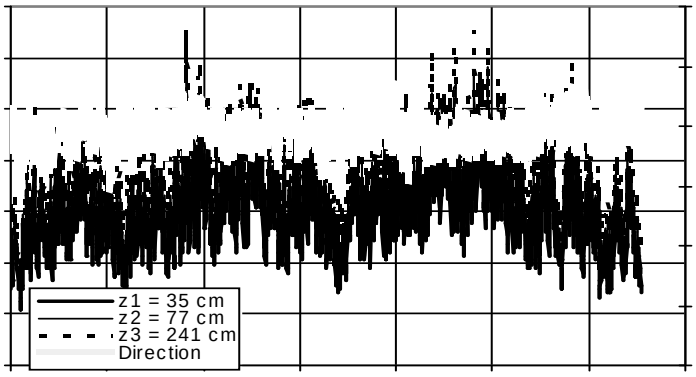

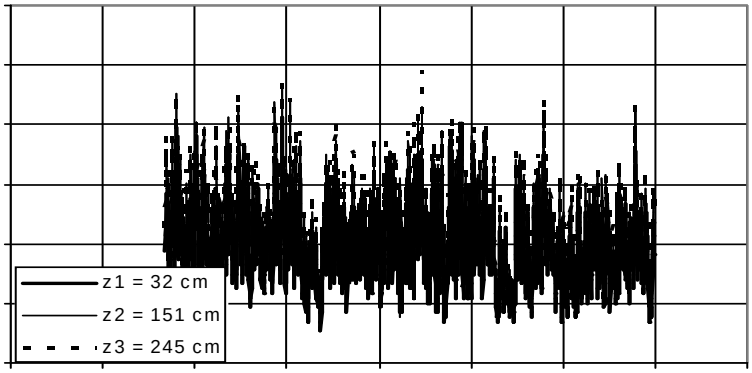

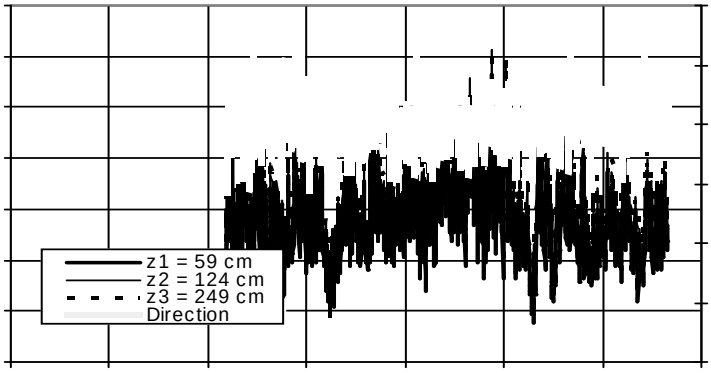

Figure 4a. Wind speed and direction data (10-second averages) collected on Round Lake on 3 March 2004.

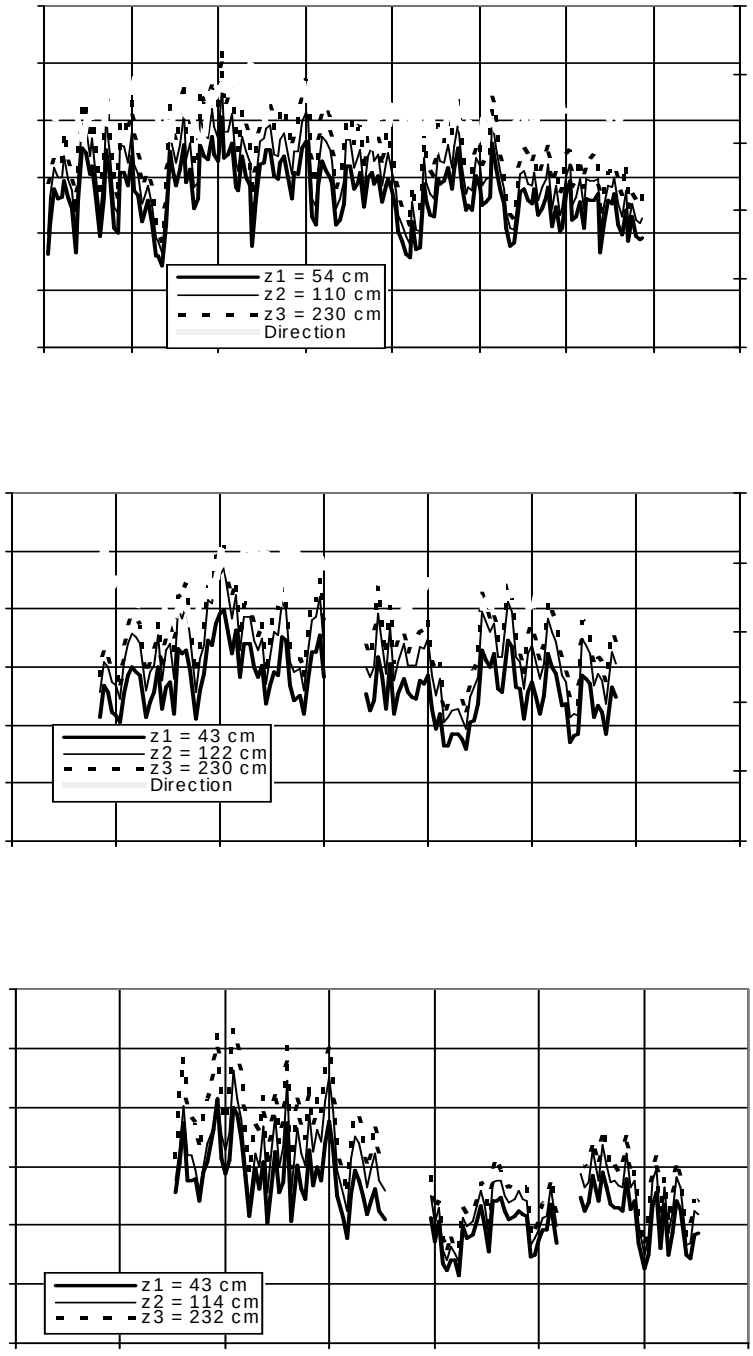

Figure 4b. Wind speed and direction data (2-minute averages) collected on Round Lake on 28 February 2004

MISSING FIGURES

Figure 4c. Wind sped and direction data (2-minute averages) collected on Round Lake on 21 February 2004.

Figure 4d. Wind speed and direction data (10-second averages) collected on Round Lake on 12 March 2004.

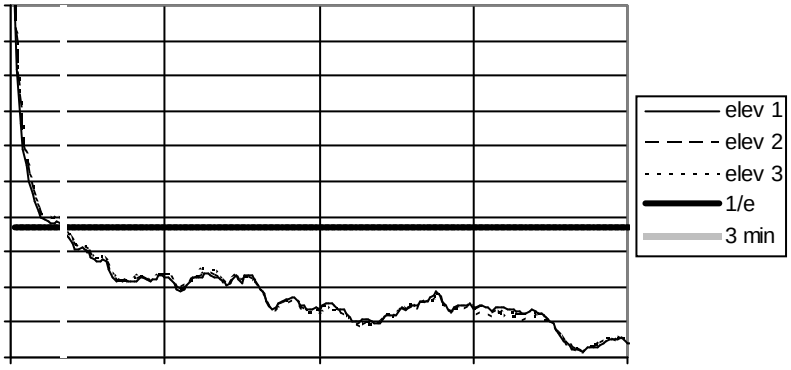

Figure 5: Examples of auto-correlograms for 10-second data from Station 1 collected at elevations of 0.4 m, 0.8 m and 2.4 m above the lake surface on 03 Mar 2004. There is no clear difference between the auto-correlograms obtained from data sets obtained at different heights.

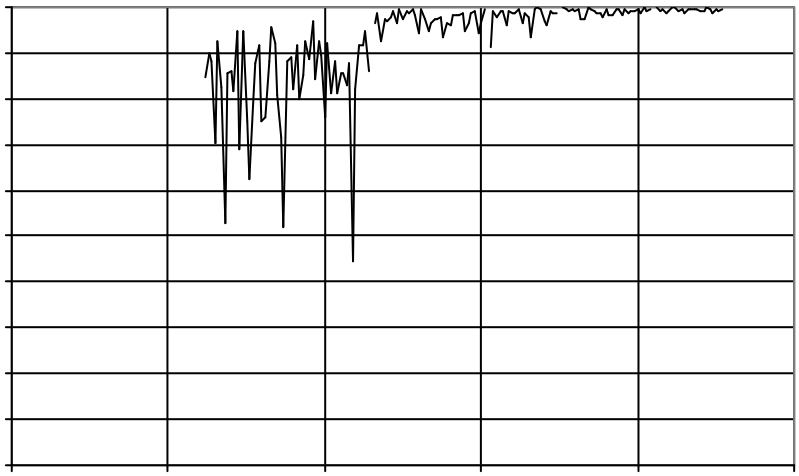

Figure 6: An example of the changing value and degree of variability of the linear regression coefficient R^2 as the mobile station is moved to locations of progressively longer fetch. The average fetch increases from approximately 10 m to approximately 250 m. Data from Round Lake, 5 Feb 2005.

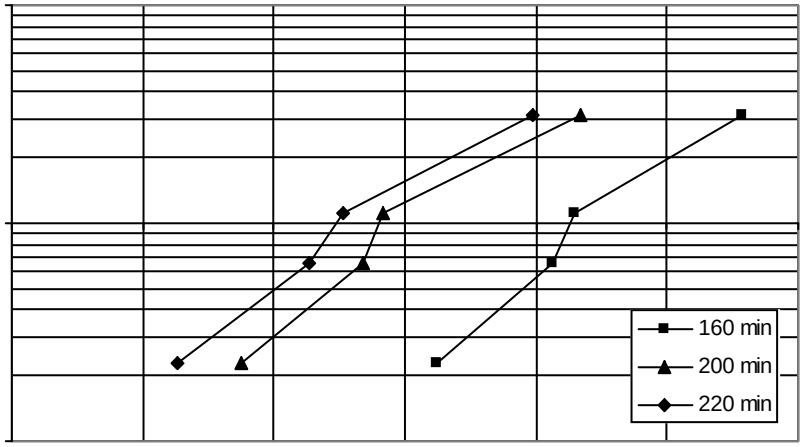

Figure 7a: Miscellaneous velocity profiles from sheltered Station 3, Lake Harriet, 23 Jan 2005. Average fetch was approximately 80m.

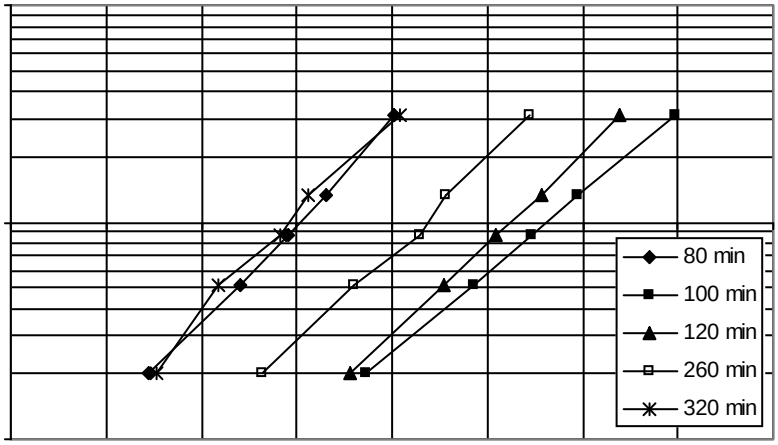

Figure 7b: Miscellaneous velocity profiles from mobile Station 2, Lake Harriet, 23 Jan 2005. For the profiles recorded at the 80, 100, and 120 minute time intervals, the fetch was approximately 440 m. The profiles shown for 260 and 320 minutes were observed at average fetches of 300 and 185 m, respectively. The linearity of the velocity profile appears to be directly related to the fetch.

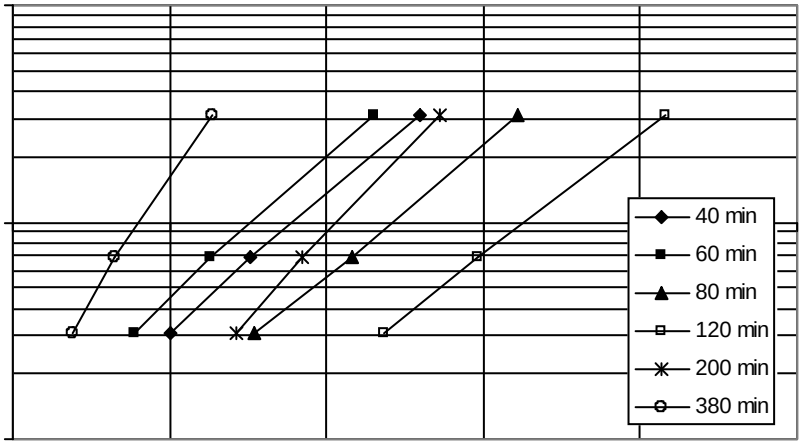

Figure 7c: Velocity profiles from far-field Station 1, Lake Harriet, 23 Jan 2005. The profiles at this downwind station are consistently and significantly closer to linear than profiles taken upwind.

MISSING FIGURES

Figure 8a. Shear velocity (Reynolds stress) obtained from sonic anemometer and from cup anemometer array at Station 2 on 3 March 2004. Sonic anemometer height is 0.93m. Average shear velocities over the measurement period are approx. 0.18 m/s and 0.09m/s, respectively.

Figure 8b. Shear velocity (Reynolds stress) obtained from sonic anemometer and from cup anemometer array at Station 1 on 12 March 2004. Sonic anemometer height is 1.07m. Average shear velocities over the measurement period are approx. 0.14 m/s and 0.07m/s, respectively.

Figure 8c. Shear velocity (Reynolds stress) obtained from sonic anemometer and from cup anemometer array at Station 3 on 12 March 2004. Sonic anemometer height is 1.28m. Average shear velocities over the measurement period are 0.13m/s and 0.07m/s, respectively.

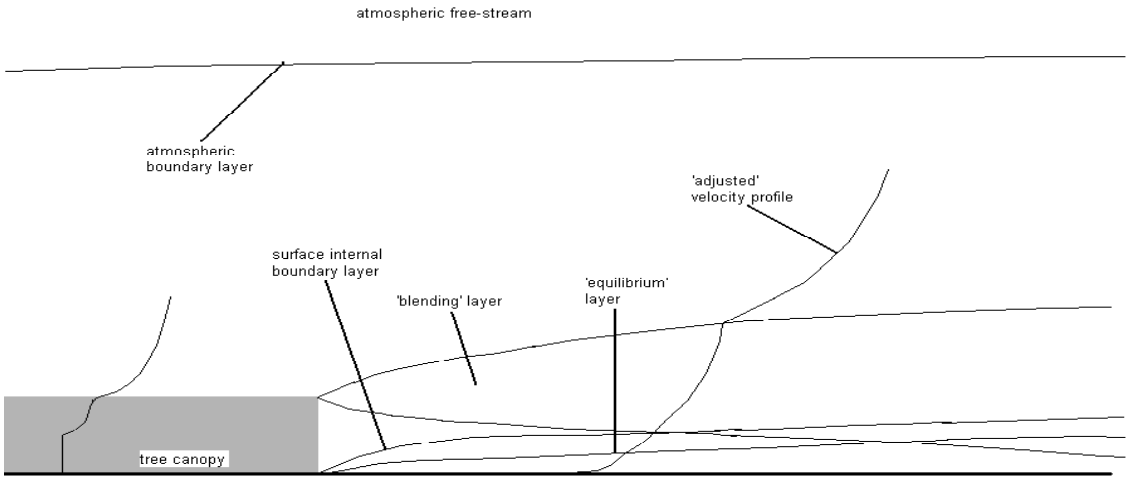

Figure 9: Schematic of hypothetical boundary layer developments and velocity profile adjustments downwind of a transition from forest to lake.

MISSING FIGURES

Figure 10. The ratios u2*/u3* at Stations 1 and 2 on 3 March 2004, computed from cup anemometer measurements at the lowest two elevations (u2*) and all three elevations (u3*). The average value of the ratios is 1.05 and 0.96 for Stations 1 and 2, respectively.

Figure 11. Velocity profiles measured with array of 5 cup anemometers (Cartesian plots).

Figure 12. Velocity profiles measured with array of 5 cup anemometers on (Semi-log plots).

Figure 13. Velocity profiles from all stations

Figure 14. Normalized shear stress ploted as a function of elevation above the water surface.

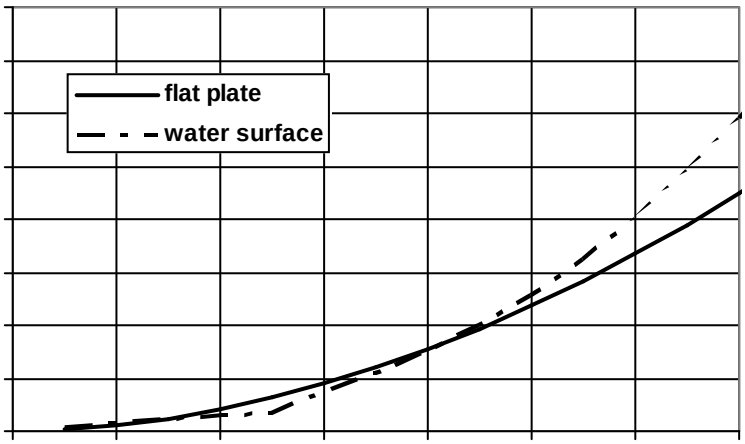

Figure A.1. Plot of wind shear stress as a function of wind speed over a flat plate and over a water surface. For the flat plate case, G(ln Rex) = 1.25. For wind speeds up to about 10 m/s, there is little discrepancy between the shear stress on a plate and the shear stress on a water surface.